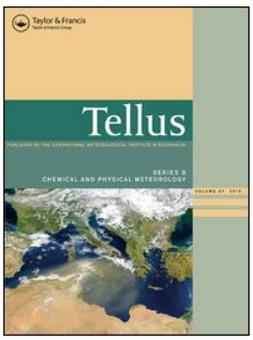

Tellus B: Chemical and Physical Meteorology

ISSN: (Print) 1600-0889 (Online) Journal homepage: https://www.tandfonline.com/loi/zelb20

Reduction of biosphere life span as a consequence of geodynamics

S. Franck, A. Block, W. Von Bloh, C. Bounama, H. J. Schellnhuber & Y. Svirezhev

To cite this article: S. Franck, A. Block, W. Von Bloh, C. Bounama, H. J. Schellnhuber & Y. Svirezhev (2000) Reduction of biosphere life span as a consequence of geodynamics, Tellus B: Chemical and Physical Meteorology, 52:1, 94-107, DOI: 10.3402/tellusb.v52i1.16085

To link to this article: https://doi.org/10.3402/tellusb.v52i1.16085

Published online: 15 Dec 2016.

Tellus (2000), 52B, 94–107
Printed in UK. All rights reserved

TELLUS
ISSN 0280–6509

Reduction of biosphere life span as a consequence of geodynamics

By S. FRANCK, A. BLOCK, W. VON BLOH, C. BOUNAMA, H. J. SCHELLNHUBER* and Y. SVIREZHEV, *Potsdam Institute for Climate Impact Research (PIK), PO Box 601203, D-14412 Potsdam, Germany*

(Manuscript received 10 August 1998; in final form 17 June 1999)

ABSTRACT

The long-term co-evolution of the geosphere–biospere complex from the Proterozoic up to 1.5 billion years into the planet's future is investigated using a conceptual earth system model including the basic geodynamic processes. The model focusses on the global carbon cycle as mediated by life and driven by increasing solar luminosity and plate tectonics. The main CO_2 sink, the weathering of silicates, is calculated as a function of biologic activity, global run-off and continental growth. The main CO_2 source, tectonic processes dominated by sea-floor spreading, is determined using a novel semi-empirical scheme. Thus, a geodynamic extension of previous geostatic approaches can be achieved. As a major result of extensive numerical investigations, the "terrestrial life corridor", i.e., the biogeophysical domain supporting a photosynthesis-based ecosphere in the planetary past and in the future, can be identified. Our findings imply, in particular, that the remaining life-span of the biosphere is considerably shorter (by a few hundred million years) than the value computed with geostatic models by other groups. The "habitable-zone concept" is also revisited, revealing the band of orbital distances from the sun warranting earth-like conditions. It turns out that this habitable zone collapses completely in some 1.4 billion years from now as a consequence of geodynamics.

1. Introduction

The fact that there has existed fluid water at the earth's surface since at least 3.8 Ga ago (Sagan and Mullen, 1972; Nisbet, 1987) is one of the main indicators of our planet's strong ability to self-regulate against external driving forces. Although the solar luminosity was significantly lower in the past, the dead end of an ice planet has been avoided. One of the main reasons for this may be the intrinsic stabilization of the coupled geosphere–biosphere system through the carbonate-silicate cycle. In spite of this surprisingly resilient character, short-term perturbations, such as a sudden increase of the carbon content of the atmosphere, may ultimately destabilize the dynamic regulation properties of the earth system in a way that paves the way towards the fate of planet Venus. A better understanding of the critical limits of the fundamental self-stabilization mechanisms is therefore crucial, especially, with respect to the unintentional global experiments humankind is presently conducting via modification of the composition of the atmosphere or fragmentation of terrestrial vegetation cover. There is increasing evidence that the main feed-back properties of the ecosphere depend not only on the capacity of its subsystems (i.e., atmosphere, hydrosphere, terrestrial and marine biosphere, pedosphere, cryosphere and lithosphere). Instead, the subsystems seem to be linked with each other in such a way that the entire system behaves as a dynamic totality, consisting of strongly interacting processes of high complexity (Ganopolski et al., 1998).

* Corresponding author.
e-mail: john@pik-potsdam.de.

The analysis of this "linkage", mainly realized through the global biogeochemical cycles, is particularly important for our ability to assess the stability of the climate system with respect to civilisatory perturbations like fossil fuel combustion. The synergetic operation of the planetary biogeochemical cycles controls a variety of earth-system properties as a result of geosphere–biosphere co-evolution over some four billion years. The main factors governing the further development are insolation, plate tectonics, photosynthesis, and atmosphere–hydrosphere interaction. As a consequence, the long-term planetary evolution defines the dynamic context in which short-term physiogenic or anthropogenic perturbations unfold. The earth system may ignore, attenuate or amplify such disturbances. Therefore, if we wish to assess the impacts of civilization-driven global change, it is mandatory to gain an understanding of how the ecosphere functions at geologic time scales: the pertinent insights will allow to define quasi-stationary boundary conditions as a systems-analytic background for studying processes at smaller temporal and spatial scales.

One of the main feedback mechanisms in the long-term evolution of the earth system is the global carbon cycle. The principal features of this cycle are important both for the past and the future of our planet. A full explanation and re-construction of the quaternary glaciation episodes, for example, seems to demand a thorough understanding of the carbon dynamics as mediated by life. "Sub specie aeternitatis", even more important questions concern the role of carbon dynamics in the determination of the overall life span of the biosphere (Lovelock and Whitfield, 1982; Caldeira and Kasting, 1992; see Schneider and Boston, 1991, for a recent review). In order to elucidate that role, the properties of all planetary CO_2 sources and sinks as a function of surface temperature, biological activity, weathering rates, sea-floor spreading, plate subduction and continental growth have to be explored in some depth. In this paper, we will explicitly take into account geodynamic properties, by way of contrast to former investigations into this issue.

The main sources of carbon are emissions from spreading zones and volcanic activities. The main sink involves the removal of CO_2 from the atmosphere by weathering processes. In extension to most of the previous studies on the carbon cycle, which refer only to present-day tectonic activities and present-day continental area, we use a general model for the thermal and degassing evolution of the earth to calculate the rate of sea-floor spreading and the growth of the continental area. As a result of our calculations, we obtain a significantly revised "terrestrial life corridor" for the earth system and a new determination of the so-called "habitable zone", i.e., the orbital region within which a planet like the earth might enjoy moderate surface temperatures and atmospheric CO_2 concentrations suitable for photosynthesis.

2. Model description

Our approach is based on improved calculations of the sea-floor spreading rate providing a measure for volcanic activities and outgassing, which represent the main sources of carbon emission. The description for weathering as the main sink of carbon contains global run-off, dissolution, biological activities (Schwartzman and Volk, 1989) and a realistic continental-growth model providing the active reaction surface for weathering.

2.1. External forcing, reservoirs, and processes

The role of weathering for the earth's climate was first described by Walker et al. (1981). In particular, the potential of weathering to stabilize the earth's surface temperature by a negative feedback mechanism that is strongly modulated by the biosphere has gained recent interest (Schwartzman and Volk, 1989; Schneider and Boston, 1991; Krumbein, 1995). Compared to subareal weathering, silicate-rock weathering on land primarily controls long-term atmospheric CO_2 content (Caldeira, 1995). The question of to what extent the biota are actually able to play an active role in stimulating the strength of the main carbon sink through weathering is crucial for an understanding of the dynamic properties of the overall earth system.

The total process of weathering embraces first the reaction of silicate minerals with carbon dioxide, second the transport of weathering products, and third the deposition of carbonate minerals in sediments. The availability of cations plays the main role in these processes and is the limiting factor in the carbonate-sediments-forming reaction (third process) between cations (Ca^{2+} and Mg^{2+}) and carbonate anions (CO_3^{2-}). Therefore,

for the mathematical formulation we have only to take into consideration the amount of released cations and their runoff (first and second process), respectively. Following Walker et al. (1981), the weathering rate F_{wr}, as a global average value, is the product of cations concentration in water (in mass per unit volume) and runoff (in volume per unit area per unit time). Therefore, the weathering rate is the mass of cations formed per unit area and unit time. Combining the direct temperature effect on the weathering reaction, the weak temperature effect on river runoff, and the dependence of weathering on soil CO_2 concentration (Walker et al., 1981; Caldeira and Kasting, 1992), the global mean silicate-rock weathering rate can be formulated via the following implicit equation:

$$\frac{F_{wr}}{F_{wr,0}} = \left(\frac{a_{H^+}}{a_{H^+,0}}\right)^{0.5} \exp\left(\frac{T_s - T_{s,0}}{13.7\ \mathrm{K}}\right). \quad (1)$$

Here the pre-factor outlines the role of the CO_2 concentration in the soil, P_{soil}; a_{H^+} is the activity of H^+ in fresh soil-water and depends on P_{soil} and the global mean surface temperature T_s. The quantities $F_{wr,0}$, $a_{H^+,0}$, and $T_{s,0}$ are the present-day values for the weathering rate, the H^+ activity, and the surface temperature, respectively. The activity a_{H^+} is itself a function of the temperature and the CO_2 concentration in the soil. The equilibrium constants for the chemical activities of the carbon and sulfur systems involved have been taken from Stumm and Morgan (1981). Note that the sulfur content in the soil also contributes to the global weathering rate, but its influence does not depend on temperature. It can be regarded as an overall weathering bias, which has to be taken into account for the estimation of the present-day value.

Eq. (1) is the key relation for our models. For any given weathering rate the surface temperature and the CO_2 concentration in the soil can be calculated self-consistently, as will be shown below. P_{soil} can be assumed to be linearly related to the terrestrial biological productivity Π (Volk, 1987) and the atmospheric CO_2 concentration P_{atm}. Thus we have

$$\frac{P_{soil}}{P_{soil,0}} = \frac{\Pi}{\Pi_0}\left(1 - \frac{P_{atm,0}}{P_{soil,0}}\right) + \frac{P_{atm}}{P_{soil,0}}, \quad (2)$$

where $P_{soil,0}$, Π_0 and $P_{atm,0}$ are again present-day values. Biologically enhanced Hadean and Archaean weathering processes would have been very different from the modern ones, although the purely inorganic processes are the same. Nevertheless, in our calculations, we assume that at least as far back to the Proterozoic, the biosphere generates the same effects as today, namely the enhancement of CO_2 concentration in soil compared to the atmospheric value.

Besides the biotic influence, which will be discussed later, the earth's surface temperature plays a dominant role in influencing the intensity of weathering as a massive carbon sink, as explained above. Caldeira and Kasting (1992) have introduced the following simplified climate model for calculating T_s: The time dependence of the solar luminosity $I(t)$ is fitted for the interval $-4.5\ \mathrm{Ga} < t < 4.77\ \mathrm{Ga}$ by the function

$$I(t) = (1 - 0.38t/4.55\ \mathrm{Ga})^{-1} 1368\ \mathrm{W\ m^{-2}}. \quad (3)$$

The energy balance between incoming and outgoing radiation is given by

$$(1 - a)I(t)/4 = \sigma T_{eff}^4, \quad (4)$$

where a is the planetary albedo, σ is the Stefan-Boltzmann constant, and T_{eff} is the effective blackbody radiation temperature which has to be increased by the greenhouse warming ΔT as function of the atmospheric carbon dioxide value P_{atm}. For an explicit formulation of the logarithmic dependence, see Caldeira and Kasting (1992). Then the global surface temperature T_s is given by the following implicit equation

$$T_s = T_{eff} + \Delta T(P_{atm}, T_s, \ldots). \quad (5)$$

This greenhouse model is valid for a very broad range of temperatures and CO_2 partial pressures ($0^\circ\mathrm{C} \leqslant T_s \leqslant 100^\circ\mathrm{C}$ and $10^{-2}\ \mathrm{ppm} \leqslant P_{atm} \leqslant 10^5\ \mathrm{ppm}$). Nevertheless, if we wish to investigate the very early terrestrial atmosphere at about 4 Ga ago that is believed to have had a P_{atm} between 10^5 and 10^7 ppm (Kasting, 1992), an extended greenhouse model working within a larger range of even higher CO_2 partial pressures is necessary. Such an improved greenhouse model is presented for example by Williams (1998).

The main role of the biosphere in the context of our model is to increase P_{soil} in relation to the atmospheric CO_2 partial pressure and proportional to the biologic productivity Π. Π is itself a function of various parameters such as water supply, photosynthetic active radiation (PHAR), nutrients (e.g., N, P and C), P_{atm}, and T_s. In the

framework of our earth system model the biological productivity Π is considered to be a function of temperature and CO_2 partial pressure in the atmosphere only. According to Liebig's principle, Π can be cast into a multiplicative form, i.e.,

$$\Pi \equiv \Pi(T_s, P_{atm}) = \Pi_{max} \cdot \Pi_T(T_s) \cdot \Pi_P(P_{atm}),$$
$$0 \leqslant \Pi_T(T_s), \quad \Pi_P(P_{atm}) \leqslant 1 \quad (6)$$

The maximum productivity, Π_{max}, is estimated to be twice the present value (Volk, 1987), thus $\Pi_{max} = 2\Pi_0$. Following Volk (1987), Michaelis-Menten hyberbolas (Richter, 1985) are suitable for describing the functional behaviour of Π_P:

$$\Pi_P(P_{atm}) = \begin{cases} \dfrac{P_{atm} - P_{min}}{P_{1/2} + (P_{atm} - P_{min})} & \text{for } P_{atm} > P_{min} \\ 0 & \text{else} \end{cases}, \quad (7)$$

where $P_{1/2} + P_{min}$ is the value at which $\Pi_P = 1/2$, and $P_{min} = 10$ ppm. Eq. (7) evidently tends to 1 for $P_{atm} \to \infty$. Experiments of plant growth under increased P_{atm} have shown an upper tolerance limit with respect to P_{atm} (Bugbee and Salisbury, 1986). Therefore, following Kump and Volk (1991), we investigate a second class of earth system models with a parabolic relation of the CO_2 dependent growth function Π_P in analogy to the Daisyworld models of Watson and Lovelock (1983) (see also Von Bloh et al. (1997)):

$$\Pi'_P(P_{atm}) = \begin{cases} 1 - \alpha \dfrac{\Pi_0}{\Pi_{max}} \left(\dfrac{P_{atm,opt}}{P_{atm,0}} - \dfrac{P_{atm}}{P_{atm,0}} \right)^2 \\ \quad \text{for } 0.2P_{atm,0} < P_{atm} < 5.66P_{atm,0} \\ 0 \quad \text{else} \end{cases}, \quad (8)$$

where $P_{atm,opt} = 2.93P_{atm,0}$ is the optimum CO_2 partial pressure for photosynthesis, $\alpha = 0.268$.

The temperature dependence of Π_T is described by a parabolic function used already by Caldeira and Kasting (1992). It has a maximum at $T_s = 25°C$:

$$\Pi_T(T_s) = \begin{cases} 1 - \left(\dfrac{T_s - 25°C}{25°C} \right)^2 & \text{for } 0°C < T_s < 50°C \\ 0 & \text{else} \end{cases}. \quad (9)$$

The resulting function $\Pi(T_s, P_{atm})$ is in any case a good description of the so-called net primary productivity (NPP) for the present biosphere. Let us emphasize that we do not consider the role of the carbon storage pool of biosphere in this paper. Within our approach, the biosphere productivity provides a measure for the biotic pump increasing P_{soil} with respect to the abiotic diffusive equilibrium between P_{atm} and P_{soil}. As a consequence, we need not take into account the net productivity containing both the production and the decomposition of biomass. On the other hand, it is still unclear whether the ansatz for $\Pi(T_s, P_{atm})$ is strictly valid for the Archaean and Proterozoic eras when biomass was produced by primitive organisms like algo-bacterial mats. Our eq. (9) can be extended to temperatures even higher than 100°C in order to incorporate hyperthermophiles (Schwartzman et al., 1993). Nevertheless, in order to facilitate comparability of our results with those found by Caldeira and Kasting (1992), we will use the temperature-dependent term given in eq. (9).

2.2. *Weathering and continental growth*

Caldeira and Kasting (1992) have calculated the life span of the biosphere under the assumption that the weathering rate F_{wr} is always equal to the present value $F_{wr,0}$. This is clearly a rather rough approximation. We call this approach the geostatic model (GSM). Berner et al. (1983) already emphasized the impact of the global weathering rate, the sea-floor spreading rate, and the continental area, respectively, on the global climate. In the framework of a dynamic-equilibrium approach for the global carbon cycle at longer time scales ($> 10^5 a$), Walker et al. (1981) first proposed a balance between the CO_2 sink in the atmosphere–ocean system and the metamorphic (plate-tectonic) source. The sources of CO_2 for the atmosphere–ocean system are sea-floor spreading at the mid-ocean ridges and back-arc or andesitic volcanism. Both processes depend on the spreading rate S (Franck et al., 1999). In most of the models for the volatile exchange between mantle and surface reservoirs (McGovern and Schubert, 1989; Franck and Bounama, 1995, 1997) the mantle degassing as the source of CO_2 for the atmosphere–ocean system is proportional to the so-called degassing volume beneath mid-ocean ridges. This degassing volume depends linearly on the spreading rate S. The sink for CO_2 in the atmosphere–ocean

system is, on the other hand, related to the weathering rate F_{wr} and the continental area A_c (available for weathering). Rock weathering happens on the continents. The weathering products are transported to the ocean and deposited exclusively as pelagic carbonates on the seafloor. In this way our model provides an upper limit for subduction of carbonates because we do not consider shallow water carbonate burial (Volk, 1989; Caldeira, 1991; Caldeira, 1992).

There is no doubt about the importance of hydrothermal reactions, especially in late Hadean and early Archaean. However, the present fluxes of basalt seawater exchange are at least one order of magnitude lower than the river dissolved fluxes from continental weathering (Wolery and Sleep, 1976, 1988). Hydrothermal fluxes are modelled proportional to the seafloor spreading rate. In the future the decreasing spreading rates result in decreasing hydrothermal fluxes. Because of our time window (Proterozoic -3.5 Ga in planetary future) we can neglect these processes. Therefore, in a well-justified linear approximation, the dynamic equilibrium of CO_2 fluxes may be expressed as a relation between dimensionless quantities (Kasting, 1984):

$$f_{wr} \cdot f_A = f_{sr}, \tag{10}$$

where $f_{wr} \equiv F_{wr}/F_{wr,0}$ is the weathering rate normalized by the present value, $f_A \equiv A_c/A_{c,0}$ is the continental area normalized by the present value, and $f_{sr} \equiv S/S_0$ is the spreading rate normalized by the present value. The ratio f_{sr}/f_A is called the "geophysical forcing ratio" (GFR). This ratio describes the influence of volcanic activities (proportional to S) and the continental area A_c on the global climate (Volk, 1987) in a nutshell.

Now we have all the means to calculate the weathering rate from geodynamical theory, and with the help of eq. (1) we can determine self-consistently the climate parameters mentioned above. Eq. (10) has been used by various authors (Berner et al., 1983; Lasaga et al., 1985; Marshall et al., 1988; Kuhn et al., 1989; Berner, 1991, 1992; Godderis and Francois, 1995) to study the influence of sea-floor spreading and continental area on weathering. Franck et al. (1999) were the first group using geodynamical theory to couple the two forcing functions of continental area and spreading, which were generally considered independently by previous geochemistry and climate modellers. This introduces an additional interaction into the system, as will be shown below.

The global carbon cycle is part of the general process of volatile exchange which has taken place throughout the earth's history. In the models of Jackson and Pollack (1987), McGovern and Schubert (1989), Williams and Pan (1992), and Franck and Bounama (1995, 1997), this volatile exchange has been studied in great detail. The main idea consists in the coupling of the thermal and the degassing history of the earth. To formalize this coupling we need a relation between the mantle heat flow, expressing the thermal history, and the sea-floor spreading rate, characterizing tectonics and volatile exchange. According to boundary layer theory, this spreading rate is given as a function of the mantle heat flow calculated by the cooling process of an oceanic plate which is approximated by the cooling of a semi-infinite halfspace. The derivation of this formula is given in the well-known textbook on geodynamics by Turcotte and Schubert (1982):

$$S(t) = \frac{q_m(t)^2 \pi \kappa A_o(t)}{[2k(T_m(t) - T_{s,0})]^2}. \tag{11}$$

Here q_m is the mean heat flow from the mantle, S is again the sea-floor spreading rate, k is the thermal conductivity, T_m is the average mantle temperature, $T_{s,0}$ is the surface temperature which is taken as the constant outer temperature of the upper boundary layer in the parameterized convection approximation, κ is the thermal diffusivity, and $A_o(t)$ is the area of ocean basins at time t. The evolution of the global average mantle heat flow is a result of the parameterized convection model. It is in good agreement with the secular mantle cooling of about 250 K within the last 3 Ga derived from the investigations of komatiites (Franck, 1998). The area of the earth's surface, A_e, is obviously the sum of $A_o(t)$ and the area of continents, $A_c(t)$, i.e.,

$$A_e = A_o(t) + A_c(t). \tag{12}$$

Eqs. (11) and (12) can be used to introduce continental-growth models into the equations for the volatile cycle.

The continental crust is especially diverse and heterogeneous, and its formation is less understood than that of the geologically relatively simple oceanic crust. Two different hypotheses have been suggested to explain the evolution of the

continental crust. The first proposes that the present continental crust formed very early in the earth's history and has been recycled through the mantle in steadily decreasing fashion such that new additions are balanced by losses, resulting in a steady-state system (Fyfe, 1978; Armstrong, 1981; Sylvester et al., 1997). The return of the continental material to the mantle and its replacement by new younger additions reduce its mean age, both of which keep the mass of the continents constant. The second hypothesis proposes crustal growth throughout geological time without recycling into the mantle. In modern studies (Taylor and McLennan, 1995), there is a growing appreciation of the observation that the continental crust grows episodically, and it is concluded that at least 60% of the crust have been replaced by the late Archaean. In the present paper we use a continental-growth model that is based on geological investigations (Condie, 1990) of the best-studied regions, North America and Europe, which formed a single land mass for most of the Proterozoic. Our empirical continental-growth model is depicted in Fig. 1. This data-based description is clearly more realistic than the theoretical models recently used by Franck et al. (1999).

As with many other authors, we assume that continental growth is the growth of the continental area. This continental area is directly related to the weathering process.

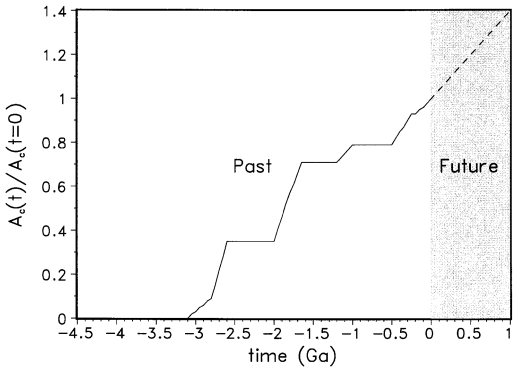

Fig. 1. Cumulative continental crust growth model derived from the best studied region, North America and Europe, according to Condie (1990). Note that crustal growth had two major pulses in the Archaean and Proterozoic. The continental area $A_c(t)$ is normalized to the present value $A_{c,0} \equiv A_c(t=0)$. Future values are estimated by a linear extrapolation (dashed line).

3. Results and discussion

In the extensive simulations we have conducted, the parameters for the present state of the earth system (e.g., $f_{wr} \equiv 1$) are used as starting values. By combining eqs. (2) to (6) with eq. (1), a relation is found which depends only on the surface temperature T_s, and the atmospheric CO_2 content P_{atm}. The next step is to use the greenhouse model of Caldeira and Kasting (1992) in order to express T_s in terms of P_{atm}. The resulting equation contains only P_{atm} as an unknown variable. The root of this equation yields the equilibrium solution of the atmospheric CO_2 content, P_{atm}. Finally, the equilibrium values of T_s, P_{soil}, and Π can be calculated. This is the solution for the present state of our earth system.

To perform the calculations at any other time, one has to use the time-dependent solar insolation (eq. (3)) and a possible change of the dimensionless weathering rate. The value of f_{wr} can be determined from the ratio of the dimensionless mid-ocean sea-floor spreading rate and the dimensionless continental area from Franck and Bounama (1995, 1997) via eq. (10). Applying the procedure described above, we run our model back to the Proterozoic. At this geological era, life had already changed from anaerobic to aerobic forms, so from that time on the biological productivity can be described by eq. (6). Starting from the present state again, we run our model 1.5 Ga into the future. This is done by extrapolating the present day continental-growth rate and by calculating the spreading rate according to Franck and Bounama (1997). In addition, we performed the whole procedure also for different orbital distances between earth and sun.

The results for the mean global surface temperature T_s and the normalized biological productivity Π/Π_0 are plotted in Figs. 2, 3, respectively. Fig. 2 compares the evolution of the mean global surface temperature from the Proterozoic up to the planetary future for the geostatic model (GSM) and for our geodynamical model (GDM). Up to 1 Ga into the future, the temperature varies only within an interval of 10°C to 40°C. This stabilization of the surface temperature is a result of the carbonate–silicate self-regulation within the earth system with respect to growing insolation as an external forcing.

In contrast to the GSM approach, the GDM

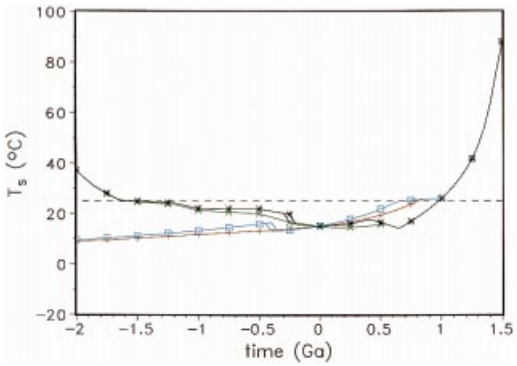

Fig. 2. Past and future variation of the mean global surface temperature $T_s(t)$ for the four employed models: GSM-asymptotic (+), GDM-asymptotic (×), GSM-parabolic (□), and GDM-parabolic (∗). The two parabolic models have multiple solutions in the past. The horizontal dashed line indicates the "optimal" biogeophysical temperature, i.e., 25°C.

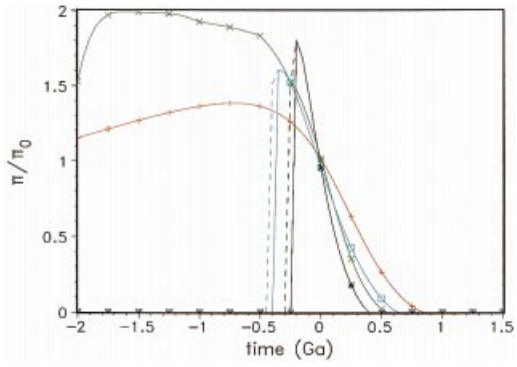

Fig. 3. Past and future variation of the normalized biological productivity Π/Π_0 for our 4 earth system models. Note that the two parabolic models have multiple solutions in the past (see also Fig. 2). The dashed branch lines correspond to backward-directed evolutions.

scheme shows a temperature stabilization at a higher level in the past and a lower one in the future (Fig. 2). This result is found for the asymptotic biospheric productivity (eq. (7)) as well as for the parabolic one described by eq. (8). Values before 2 Ga ago are not shown because at these times the GDM gives atmospheric CO_2 concentrations higher than 10^5 ppm. Under the latter conditions the greenhouse model employed is not valid. Nevertheless, both models show a good stabilization of the mean global surface temperature T_s against increasing insolation. In the far future, near 1 Ga from now, all curves converge and show a strong increase in T_s to almost 100°C. All higher forms of life, especially the photosynthesis-based biosphere, will certainly be extinguished at this time. This kind of sensitivity was also discussed for other continental-growth models in previous papers (Franck and Bounama, 1997; Franck et al., 1999).

During the long-term evolution of the earth system, the development of the normalized biological productivity (Fig. 3) shows a remarkably different behaviour for the asymptotic and the parabolic models, respectively.

Because of the chosen set of parameters used in eq. (8), both parabolic models (GSM and GDM) have zero productivities for times earlier than 500 Ma before present. This obviously contradicts the geological record. Therefore, in the following, we will restrict ourselves to asymptotic models only. In the past, these models generate higher values of Π/Π_0 than today. Our favoured model, the GDM-asymptotic model, calculates twice the present biological productivity for most of the Proterozoic. This seems reasonable because of the higher mean global surface temperatures at that time. As continental growth starts late in our GDM-asymptotic model, the latter generates a strong increase in the biological productivity in the Proterozoic. This model also provides the shortest life span of the photosynthesis-based biosphere — nearly 300 Ma shorter than the corresponding GSM-asymptotic model!

Fig. 4 shows the atmospheric carbon content over geologic time from the Hadean to the planetary future for the two asymptotic models. In the dashed region of Fig. 4 no photosynthesis is possible because of inappropriate temperature or atmospheric carbon content. The non-dashed region is the "terrestrial life corridor (TLC)". Formally, the life corridor in the (P_{atm}, T_s)-domain is defined as

$$\mathrm{TLC} := \{(P_{atm}, T_s) \,|\, \Pi(P_{atm}, T_s) > 0\}\,. \tag{13}$$

For the asymptotic model, we have (inserting eqs. (6), (7), and (9) into eq. (13)):

$$\mathrm{TLC} = \{(P_{atm}, T_s) \,|\, 0°\mathrm{C} < T_s < 50°\mathrm{C} \wedge P_{atm} > P_{min}\}\,. \tag{14}$$

It is possible to map TLC in different parameter spaces. For instance, T_s can be substituted with the help of the greenhouse model by P_{atm}.

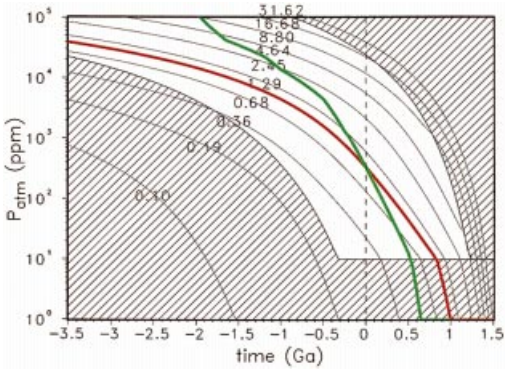

Fig. 4. Evolution of the atmospheric carbon content as described by the models GSM-asymptotic (red line) and GDM-asymptotic (green line). The terrestrial life corridor (eq. (14)) is identical to the non-dashed region. The plotted isolines are the solutions of GSM-asymptotic for the indicated fixed values of the normalized weathering rate f_{wr}.

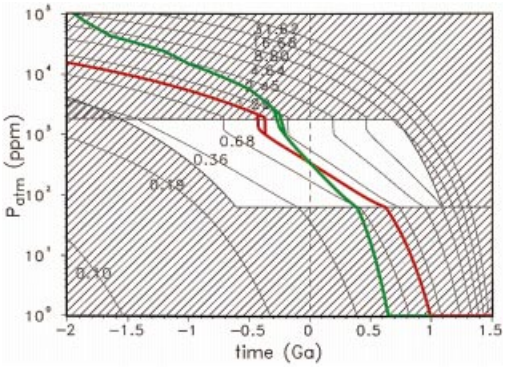

Fig. 5. Evolution of the atmospheric carbon content as described by the models GSM-parabolic (red line) and GDM-parabolic (green line). The terrestrial life corridor for the parabolic model is defined by $\mathrm{TLC}' = \{(P_{atm}, T_s) \mid 0°C < T_s < 50°C \wedge 0.2P_{atm,0} < P_{atm} < 5.66P_{atm,0}\}$ and is identical to the non-dashed region. The plotted isolines have the same meaning as in Fig. 4.

Therefore, TLC can be depicted in the (P_{atm}, t)-domain, as shown in Fig. 4. The reference model GSM is based on a weathering rate that is always equal to the present-day rate $F_{wr}/F_{wr,0} = 1$. The GDM takes into account the influence of a growing continental area and the changing spreading rate on weathering. The GDM has higher weathering rates for the past (i.e., $F_{wr}/F_{wr,0} > 1$). This can be explained easily with the help of eq. (10), because in the geological past we had higher spreading rates f_{sr} and a smaller continental area f_A. In the planetary future we find the reversed situation: lower spreading rates and higher continental area will reduce the atmospheric carbon content, and this is the reason why the biosphere's life span is significantly shorter because photosynthesis can persist only down to the critical level of 10 ppm atmospheric CO_2 concentration. As mentioned above, the GDM model does not work at atmospheric CO_2 concentrations higher than 10^5 ppm, and therefore the model fails on time scales of about 2 Ga ago. Compared to the smooth curve of the GSM-asymptotic model, our favoured model (GDM-asymptotic) provides a curve with a certain structure that is directly related to the step-like continental growth shown in Fig. 1.

The life corridor for the two parabolic models is plotted in Fig. 5. As already mentioned above, these models do not work very well for the past because the upper boundary for the atmospheric CO_2 content is rather low, between 10^3 and 10^4 ppm. Nevertheless, both curves show the phenomenon of bistability in the Phanerozoic. Dependent on the time direction, there are different evolutionary paths in the diagram. Such a hysteresis, in a much more pronounced form, can also be calculated for the Daisyworld model class (von Bloh et al., 1997). Similar effects were discussed by Kump and Volk (1991). They found both bistability and insufficient conditions for life for times of more than 100 Ma ago for the parabolic model, which is clearly not realistic.

Besides calculating the TLC, i.e., the evolution of atmospheric carbon regimes supporting photosynthetis-based life in time, we calculated the behaviour of our virtual earth system at various distances from the sun, using different insolations. Hart (1978, 1979) calculated the evolution of the terrestrial atmosphere over geologic time by varying the distance from the sun. In his approach, the habitable zone (HZ) is the region within which an earth-like planet might enjoy moderate surface temperatures needed for advanced life forms. Kasting et al. (1993) defined the HZ of an earth-like planet as the region where liquid water is present at the surface. According to this definition the inner boundary of the HZ is determined by the loss of water via photolysis and hydrogen escape. Kasting et al. (1993) propose three

definitions of the outer boundary of the HZ. All of them are connected to a surface-temperature limit of 273 K. This is in agreement with our definition of the low-temperature boundary of the biological productivity.

According to Kasting et al. (1993) the outer boundary of the HZ is determined by CO_2 clouds that attenuate the incident sunlight by Rayleigh scattering. The critical CO_2 partial pressure for the onset of this effect is about 5 to 6 bar (Kasting, personal communication, 1999). On the other hand, the effects of CO_2 clouds have been challenged recently by Forget and Pierrehumbert (1997). CO_2 clouds have the additional effect of reflecting the outgoing thermal radiation back to the surface. In this way, they could have extended the size of the HZ in the past.

Hart (1978, 1979) found that the HZ between runaway greenhouse and runaway glaciation is surprisingly narrow for G2 stars like our sun: $R_{\text{inner}} = 0.958$ AU, $R_{\text{outer}} = 1.004$ AU (AU = astronomical unit). A main disadvantage of these calculations is the neglect of the negative feedback between atmospheric CO_2 content and mean global surface temperature discovered later by Walker et al. (1981). The implementation of this feedback by Kasting et al. (1988) provides an almost constant inner boundary ($R_{\text{inner}} = 0.95$ AU) but a remarkable extension of the outer boundary beyond Martian distance ($R_{\text{outer}} = 1.5$ AU). Later, Kasting et al. (1993) and Kasting (1997) recalculated the HZ boundaries as $R_{\text{inner}} = 0.95$ AU and $R_{\text{outer}} = 1.37$ AU.

In a recent paper, Williams and Kasting (1997) investigated the problem of habitable planets with high obliquities with the help of an energy-balance climate model. In their two-dimensional model R_{outer} shifts to ≈ 1.40 AU. In our approach, the HZ for an earth-like planet is the region within which the biological productivity is greater than zero. This is the region where the surface temperature stays between 0°C and 50°C and the atmospheric CO_2 content is higher than 10 ppm suitable for photosynthetis-based life. The term "earth-like" explicitly implies also the occurrence of plate tectonics. In order to assess the HZ, the life corridor is calculated by varying the distance of our earth-like planet to the sun for various time steps in the past, the present, and the future. Fig. 6 shows the results for the present state of the earth system.

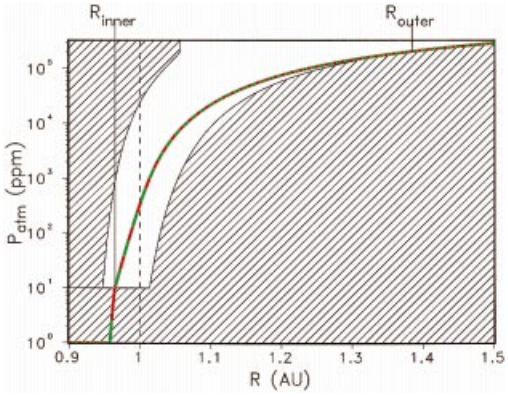

Fig. 6. Present habitable zone (non-dashed region) for GSM-asymptotic (red) and GDM-asymptotic (green). The two models provide identical answers as they are both fitted to the same present-day parameters. Present inner and outer boundaries are determined as $R_{\text{inner}} = 0.97$ AU and $R_{\text{outer}} = 1.39$ AU, respectively.

In this case, GSM and GDM give identical curves because both models are fitted to the same present parameters. We find $R_{\text{inner}} = 0.97$ AU, so our earth system is even closer to a runaway greenhouse effect than in the calculations of Hart (1979) and Kasting et al. (1988). The outer boundary is extended in comparison to the model of Hart (1979), but not beyond the Martian distance ($R_{\text{outer}} = 1.39$ AU). Despite the different ansatz, our results are comparable to those found by Kasting et al. (1993), Kasting (1997), and Williams and Kasting (1997).

In the planetary future at 0.5 Ga from now, the situation has changed dramatically (Fig. 7): the geodynamic earth-system model GDM predicts that the lower boundary for atmospheric CO_2 concentration has been reached already ($R_{\text{inner}} = 1.00$ AU), and the boundary for a runaway glaciation has moved significantly inward ($R_{\text{outer}} = 1.17$ AU). Our results for the estimation of the HZ for all times are summarized in Fig. 8, where we have plotted the width and position of the HZ for the GSM and GDM variants over time.

For the geostatic case (GSM) the width of the HZ slightly increases and shifts outward over time. In about 800 Ma the inner boundary R_{inner} reaches the earth distance from the sun ($R = 1$ AU) and the biosphere ceases to exist, as already found above for this model. Our geodynamic model shows both a shift and a narrowing of the HZ:

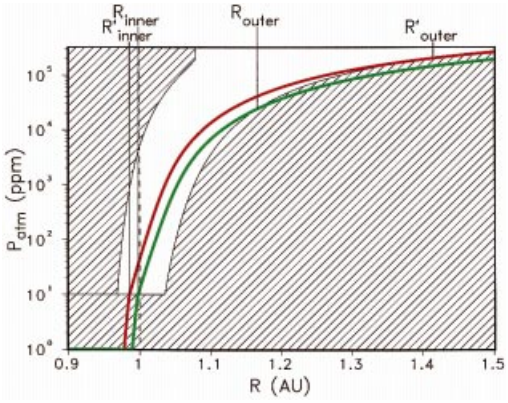

Fig. 7. The habitable zone (non-dashed region) for an earth-like planet in the "near" future (0.5 Ga). For GDM-asymptotic (green line) the respective boundaries are $R_{\text{inner}} = 1.0$ AU and $R_{\text{outer}} = 1.17$ AU. Because R_{inner} will exactly coincide with the actual distance of planet earth from the sun (1 AU), the life span of the biosphere will end at this time. For GSM-asymptotic (red line) the respective boundaries are $R'_{\text{inner}} = 0.99$ AU and $R'_{\text{outer}} = 1.41$ AU.

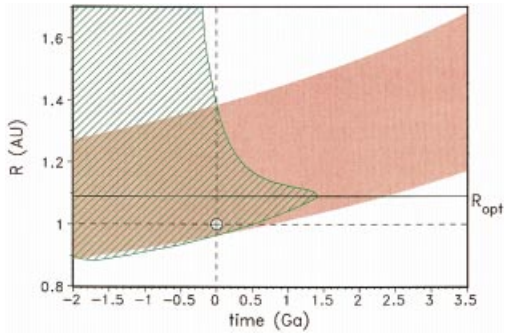

Fig. 8. Evolution of the habitable zone (HZ) for GSM-asymptotic (red line) and GDM-asymptotic (green line). Note that for GSM-asymptotic the HZ has a slightly increasing width and shifts outward from the sun. The HZ for our favoured model, GDM-asymptotic, is both shifting and narrowing over geologic time, terminating life definitely at 1.4 Ga. The optimum position for an earth-like planet would be at $R_{\text{opt}} = 1.08$ AU. In this case the life span of the biosphere would realize the maximum life span, i.e., the above-mentioned 1.4 Ga. This figure is the main finding of our investigation.

the inner boundary R'_{inner} reaches the earth distance in about 500 Ma from now in correspondence with the shortening of the life span of the biosphere by about 300 Ma as compared to the geostatic model. In the GDM, the outer boundary R_{outer} decreases in a strong nonlinear way. This result is in contrast to the GSM and to the results of Kasting et al. (1993) and Kasting (1997). Since our criteria for the HZ is defined using biological productivity alone, the critical boundaries can be extended for the temperature from 50°C to 100°C or higher. But our results show that the inner boundary of the HZ is determined by the 10 ppm limit (Figs. 6, 7) and the outer boundary by the 0°C limit.

Of course, there may exist chemolithoautotrophic hyperthermophiles that might survive even in a future of higher temperatures, rather independently of atmospheric CO_2 pressures. But all higher forms of life would certainly be eliminated under such conditions. Our biosphere model is actually only relevant to photosynthesis-based life. Therefore, in the time span under consideration, the upper temperature does not affect the results for TLC and HZ, respectively.

The main objective of our paper is to generate model results for the dependence of the biosphere life span on the sea-floor spreading rate and the history of continent growth. Therefore, sensitivity tests based on the variations of these geodynamics entities have been performed. In Fig. 9, the ensemble of alternative continental-growth models is sketched. The linear and the delayed growth models reflect the simplest theoretical assumptions (Franck and Bounama, 1997). The model of Reymer and Schubert (1984) is based on the assumption of an approximately constant

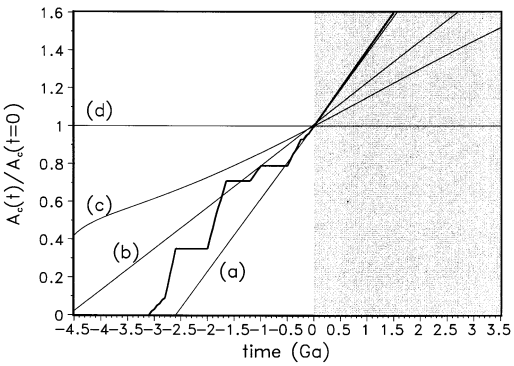

Fig. 9. Normalized continental area $A_c(t)/A_C(t=0)$ as a consequence of the following continental-growth models: (a) delayed growth, (b) linear growth, (c) Reymer and Schubert, (d) constant area. The thick line indicates the Condie model (Fig. 1).

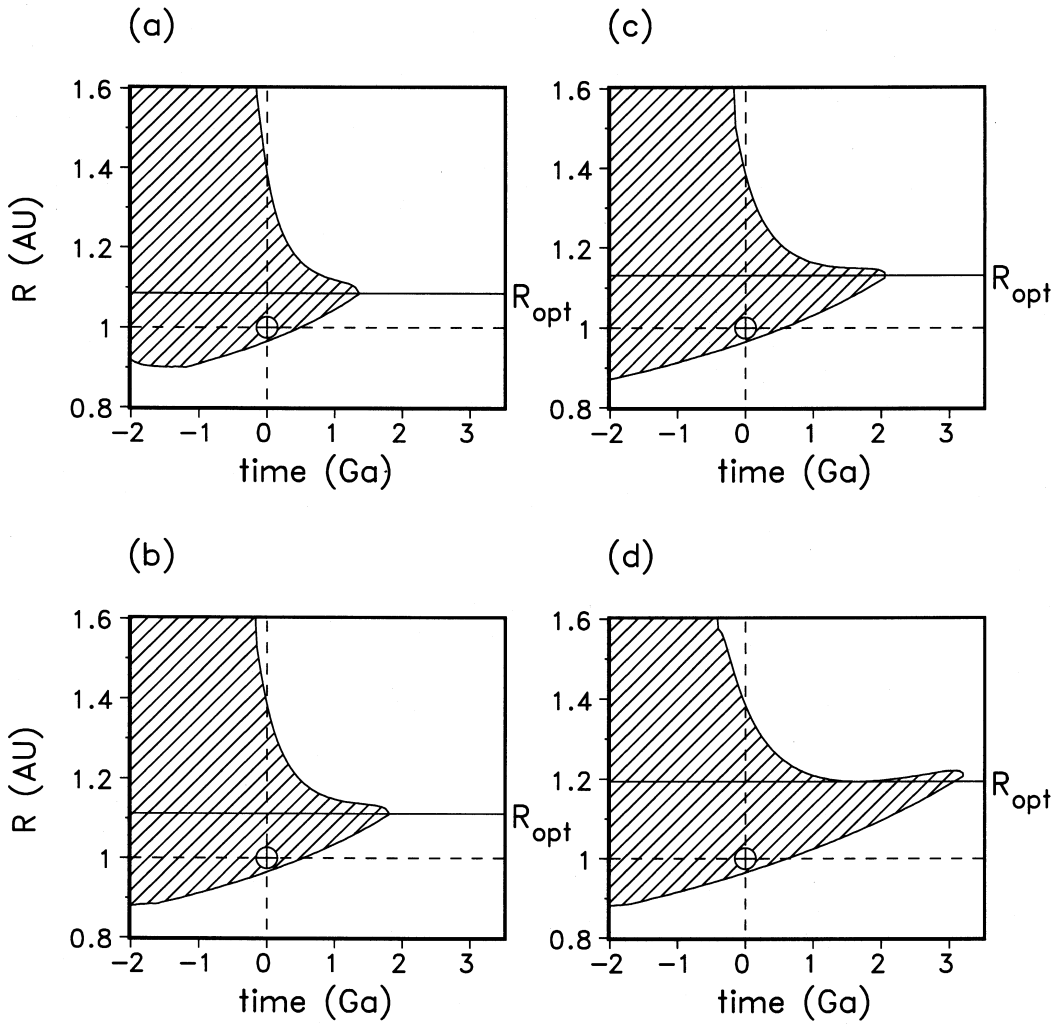

Fig. 10. Habitable zones of the GDM-asymptotic for the four alternative continental-growth models: (a) delayed growth, (b) linear growth, (c) Reymer and Schubert, (d) constant area. Obviously, the so-calculated HZs do not differ in their qualitative behaviour. The biosphere life span varies only slightly in magnitude and is always shorter than in the geostatic case (GSM). Exact values for the biosphere life span, the optimum distance, and the maximum life span, respectively, can be found in Table 1.

continental freeboard. For all of these models surface temperature, CO_2 history, and biological productivity have been already investigated by Franck et al. (1999) in a recent study. Furthermore, we added a model with constant continental area which seems to be in contrast to geological records. Therefore, this geodynamic scenario is the most unrealistic one. In all cases, the spreading rates are calculated with the help of eq. (11).

Fig. 10 summarizes the results for the HZs for the additional four continental-growth scenarios indicated in Fig. 9. It is obvious that in all cases the life span of the biosphere is significantly shorter than in the GSM and the magnitude remains approximately the same for all alternatives (Table 1). The optimum distances for an earth-like planet vary slightly between 1.09 and 1.21 AU. The maximum life span at the optimum distance varies between

1.35 and 2.05 Ga in cases a, b, and c, respectively, evidently increasing with decreasing continental-growth rate. In the most unrealistic case without continental growth but geodynamics, i.e., scenario d, the maximum life span is extended to 2.98 Ga.

The comparison of Figs. 8, 10 demonstrates that the character of of the HZ remains similar in all the GDM cases. There are only minor differences in the quantitative results (Table 1). The results for the geodynamic model with continental growth according to Condie (1990) are well within the range of the overall model ensemble. Therefore, we favour the Condie continental-growth models as it is directly related to the geological record.

Our results for life corridors and habitable zone are certainly relevant for the overall debate on sustainable development and geocybernetics (Schellnhuber and Kropp, 1998). Regarding the "ecological niche for civilization" on earth, we can learn from Fig. 8 that within the framework of our favoured model (GDM-asymptotic) the "optimal" planetary distance from the sun would be about 1.08 AU. At such a distance the self-regulation mechanism would work ideally against external forcing arising from increasing solar insolation or other perturbations, and the life span of the biosphere would be extended to 1.4 Ga. But after that time, the biosphere will definitely cease to exist. Our findings are also relevant to the search for habitable zones around other main-sequence stars (Hart, 1979).

Finally, we want to emphasize that all predictions about the long-scale evolution of the earth system include uncertainties. These uncertainties are mainly related to inherent imperfections in modelling single components of the earth system. Nevertheless, we are convinced that our main conclusions, especially about the shortening of the life span and the narrowing of the HZ, are qualitatively correct. A more detailed analysis of the response of the earth system against perturbations at various time scales requires a dynamic extension of the present models, however. Such an investigation needs particularly the analysis of possible accelerations and inertial effects of the global weathering rate. This will be part of future work.

Table 1. *Life span of the biosphere, optimum distance to the sun, R_{opt}, and maximum life span at R_{opt}, respectively, for the five different continental-growth models*

Continental growth model	Biosphere life span (Ga)	R_{opt} (AU)	Maximum life span (Ga)
delayed growth	0.48	1.09	1.35
Condie	0.48	1.08	1.40
linear growth	0.53	1.11	1.80
Reymer and Schubert	0.58	1.13	2.05
constant area	0.63	1.19	2.98

4. Acknowledgements

This work was supported by the German Science Foundation (DFG, grant number IIC5-Fr910/9-1,2). We would like to thank Prof. G. Zavarzin (Russian Academy of Sciences, Moscow) and the three reviewers for helpful discussions and their constructive remarks.

REFERENCES

Armstrong, R. L. 1981. The persistent myth of the crustal growth. *Aust. J. Earth Sci.* **38**, 613–630.

Berner, R. A. 1991. A model for atmospheric CO_2 over Phanerozoic time. *Am. J. Sci.* **291**, 339–376.

Berner, R. A. 1992. Weathering, plants, and long-term carbon cycle. *Geochim. Cosmochim. Acta* **56**, 3225–3231.

Berner, R. A., Lasaga, A. C. and Garrels, R. M. 1983. The carbonate–silicate geochemical cycle and its effects on atmospheric carbon dioxide over the past 100 million years. *Am. J. Sci.* **283**, 641–683.

Bugbee, B. G. and Salisbury, F. B. 1986. Studies on maximum yield of wheat for the controlled environments of space. In: *Controlled ecological life support systems: CELSS 1985 Workshop*, ed. R. D. MacElroy, N. Y. Martello, D. T. Smernoff. NASA-TM-88215, National Aeronautics and Space Administration, Washington DC, pp. 447–486.

Caldeira, K. 1991. Continental-pelagic carbonate partitioning and the global carbonate-silicate cycle. *Geology* **19**, 204–206.

Caldeira, K. 1992. Enhanced cenozoic chemical weathering and the subduction of pelagic carbonate. *Nature* **357**, 578–581.

Caldeira, K. 1995. Long-term control of atmospheric carbon dioxide — low-temperature seafloor alteration or terrestrial silicate-rock weathering. *Am. J. Sci.* **295**, 1077–1114.

Caldeira, K. and Kasting, J. F. 1992. The life span of the biosphere revisited. *Nature* **360**, 721–723.

Condie, K. C. 1990. Growth and accretion of continental crust: inferences based on Laurentia. *Chem. Geology* **83**, 183–194.

Forget, F. and Pierrehumbert, R.T. 1997. Warming early Mars with carbon dioxide clouds that scatter infrared radiation. *Science* **278**, 1273–1276.

Franck, S. 1998. Evolution of the global heat flow over 4.6 Gyr. *Tectonophysics* **291**, 9–18.

Franck, S. and Bounama, Ch. 1995. Effects of water-dependent creep rate on the volatile exchange between mantle and surface reservoirs. *Phys. Earth Planet. Inter*. **92**, 57–65.

Franck, S. and Bounama, Ch. 1997. Continental growth and volatile exchange during Earth's evolution. *Phys. Earth Planet. Inter*. **100**, 189–196.

Franck, S., Kossacki, K. and Bounama, Ch. 1999. Modelling the global carbon cycle for the past and future evolution of the Earth system. *Chem. Geology* **159**, 305–317.

Fyfe, W. D. 1978. Evolution of the earth's crust: modern plate tectonics to ancient hot spot tectonics? *Chem. Geol.* **23**, 89–114. Ganopolski, A., Kubatzki, C., Claussen, M., Brovkin, V. and Petoukhov, V. 1998. Vegetation–atmosphere–ocean interaction on climate during Mid-Holocene. *Science* **280**, 1916–1919.

Goddéris, Y. and Francois, L. M. 1995. The cenozoic evolution of the strontium and carbon cycle: relative importance of continental erosion and mantle exchanges. *Chem. Geology* **126**, 169–190.

Hart, M. H. 1978. The evolution of the atmosphere of the Earth. *Icarus* **33**, 23–39.

Hart, M. H. 1979. Habitable zones about main sequence stars. *Icarus* **37**, 351–357.

Jackson, M. J. and Pollack, H. N. 1987. Mantle devolatilization and convection: implications for the thermal history of the Earth. *Geophys. Res. Lett*. **14**, 7, 737–740.

Kasting, J. F. 1984. Comments on the BLAG model: the carbonate–silicate geochemical cycle and its effect on atmospheric carbon dioxide over the past 100 million years. *Am. J. Sci.* **284**, 1175–1182.

Kasting, J. F. 1992. *The proterozoic biosphere*. Schopf, J. W., Klein, C. (eds.). Cambridge University Press, Cambridge, pp. 165–168.

Kasting, J. F. 1997. Habitable zones around low mass stars and the search for extraterrestrial life. *Origins of Life* **27**, 291–307.

Kasting, J. F., Toon, O. B. and Pollack, J. B. 1988. How climate evolved on the terrestrial planets. *Sci. Am.* **258**,2, 46–53.

Kasting, J. F., Whitmire, D. P. and Reynolds, R. T. 1993. Habitable zones around main sequence stars. *Icarus* **101**, 108–128.

Krumbein, W. E. 1995. A neglected carbon sink? Biodegradation of rocks. In: *Microbial diversity and ecosystem function.* Allsopp, D., Colwell, R. R. and Hawksworth, D. L. (eds.). CAB International, Wallingford.

Kuhn, W. R., Walker, J. C. G. and Marshall, H. G. 1989 The effect on Earth's surface temperature from variations in rotation rate, continent formation, solar luminosity, and carbon dioxide. *J. Geophys. Res.* **94**, 11,129–11,136.

Kump, L. R. and Volk, T. 1991. Gaia's garden and BLAG's greenhouse: global biogeochemical climate regulation. In: *Scientists on Gaia*, ed. S. H. Schneider and P. J. Boston. MIT Press, Cambridge, 191–199.

Lasaga, A. C., Berner, R. A. and Garrels, R. M. 1985. An improved geochemical model of atmospheric CO_2 fluctuation over the past 100 million years. In: The carbon cycle and atmospheric CO_2: natural variations Archaean to present. *Geophys. Monograph* **32**, ed. E. T. Sundquist and W. S. Broecker. AGU, Washington DC, pp. 397–441.

Lovelock, J. E. and Whitfield, M. 1982. Life span of biosphere. *Nature* **296**, 561–563.

Marshall, H. G., Walker, J. C. G, and Kuhn, W. R. 1988. Long-term climate change and the geochemical cycle of carbon. *J. Geophys. Res.* **93**, 781–801.

McGovern, P. J. and Schubert, G. 1989. Thermal evolution of the Earth: effects of volatile exchange between atmosphere and interior. *Earth Planet. Sci. Lett*. **96**, 27–37.

Nisbet, E. G. 1987.*The young Earth: an introduction to Archean geology*. Allen & Unwin Inc., London, pp. 402.

Reymer, A. and Schubert, G. 1984. Phanerozoic addition rates of the continental crust and crustal growth. *Tectonics* **3**, 63–67.

Richter, O. 1985. *Simulation des Verhaltens ökologischer Systeme: Mathematische Methoden und Modelle*. Verlag Chemie, Weinheim, pp. 219.

Sagan, C. and Mullen, G. 1972. Earth and Mars: evolution of atmospheres and surface temperatures. *Science* **177**, 52–56.

Schellnhuber, H.-J. and Kropp, J. 1998. Geocybernetics: controlling a complex dynamic system under uncertainty. *Naturwissenschaften* **85**, 411–425.

Schneider, S. H. and Boston, P. J. (eds.) 1991. *Scientists on Gaia*. MIT Press, Cambridge, pp. 550.

Schwartzman, D., McMenamin, M. and Volk, T. 1993. Did surface temperatures constrain microbial evolution? *BioSci.* **43**, 390–393.

Schwartzman, D. W. and Volk, T. 1989. Biotic enhancement of weathering and the habitability of earth. *Nature* **340**, 457–460.

Stumm, W. and Morgan, J. J. 1981. *Aquatic chemistry*. Wiley, New York, 780 pp.

Sylvester, P. J., Campbell, I. H. and Bowyer, D. A. 1997. Niobium/uranium evidence for early formation of the continental crust. *Science* **275**, 521–523.

Taylor, S. R. and McLennan, S. M. 1995. The geological evolution of the continental crust. *Rev. Geophysics* **33**, 641–265.

Turcotte, D. L. and Schubert, G. 1982. *Geodynamics*. Wiley, New York, 450 pp.

Volk, T. 1987. Feedbacks between weathering and atmospheric CO_2 over the last 100 million years. *Am. J. Sci.* **287**, 763–779.

Volk, T. 1989. Sensitivity of climate and atmospheric CO_2 deep-ocean and shallow-ocean carbonate burial. *Nature* **337**, 637–640.

Von Bloh, W., Block, A. and Schellnhuber, H.-J. 1997. Self-stabilisation of the biosphere under global change: a tutorial geophysiological approach. *Tellus* **49B**, 249–262.

Walker, J. C. G., Hays, P. B. and Kasting, J. F. 1981. A negative feedback mechanism for the long-term stabilization of Earth's surface temperature. *J. Geophys, Res.* **86**, 9776–9782.

Watson, A. J. and Lovelock, J. E. 1983. Biological homeostasis of the global environment: the parable of Daisyworld. *Tellus* **35B**, 284–289.

Williams, D. M. 1998. *The stability of habitable planetary environments*. Thesis, Pennsylvania State University.

Williams, D. M. and Kasting, J. F. 1997. Habitable planets with high obliquities. *Icarus* **129**, 254–267.

Williams, D. R. and Pan, V. 1992. Internally heated mantle convection and the thermal and degassing history of the Earth. *J. Geophys. Res.* **97**, B6, 8937–8950.

Wolery, T. J. and Sleep, N. H. 1976. Hydrothermal circulation and geochemical flux at mid-ocean ridges. *J. Geol.* **84**, 249–275.

Wolery, T. J. and Sleep, N. H. 1988. Interactions of geochemical cycles with the mantle. In: *Chemical cycles in the evolution of the earth*, eds. C. B. Gregor, R. M. Garrels, F. T. Mackenzie, J. B. Maynard. Wiley & Sons, New York, pp. 77–103.